Formation of InGaAs quantum dots in the body of AlGaAs nanowires via molecular-beam epitaxy

© R.R. Reznik[1], V.O. Gridchin[1,2,3], K.P. Kotlyar[1,2,3], A.I. Khrebtov[2], E.V. Ubyivovk[1], S.V. Mikushev[1], D. Li[4], R. Radhakrishnan[4], J.F. Neto[4], N. Akopian[4], G.E. Cirlin[1,2,3]

[1] St. Petersburg State University,
199034 St. Petersburg, Russia
[2] Alferov University,
194021 St. Petersburg, Russia
[3] Institute for Analytical Instrumentation
of the Russian Academy of Sciences,
190103 St. Petersburg, Russia
[4] DTU Fotonik,
2800 Kongens Lyngby, Denmark

E-mail: moment92@mail.ru

Received March 2, 2022
Revised March 25, 2022
Accepted March 25, 2022

The results of experimental studies on the synthesis by molecular-beam epitaxy of AlGaAs nanowires with InGaAs quantum dots are presented. It was shown that, as in the case of the InP/InAsP material system, the formation of predominantly two objects is observed in the body of AlGaAs nanowire: InGaAs quantum dot due to axial growth and InGaAs quantum well due to radial growth. It is important to note that the grown nanostructures were formed predominantly in the wurtzite crystallographic phase. The results of the grown nanostructures physical properties studies indicate that they are promising for moving single-photon sources to the long-wavelength region. The proposed technology opens up new possibilities for integration direct-gap III−V materials with a silicon platform for various applications in photonics and quantum communications.

Keywords: semiconductors, nanowires, quantum dots, III−V compounds, silicon, molecular-beam epitaxy.

DOI: 10.21883/SC.2022.07.54653.16

1. Introduction

At present, semiconductor nanostructures based on compounds III−V attract increased interest of researchers due to their unique properties and the development of modern methods of synthesis [1–3]. Of particular interest for creating optoelectronic applications are nanostructures of combined dimensions, such as quantum dots (QD) in the body of nanowhiskers (NWs) [4–8]. Unlike self-organized QDs on mismatched surfaces [9], the diameter, height, and density of such QDs are determined by the NW diameter, growth time, and NW density, respectively. It is important to note that, due to the effective relaxation of mechanical stresses on the side faces of NWs, such hybrid nanostructures can be synthesized on the silicon surface. In our previous works, we demonstrated the possibility of growing AlGaAs NWs with GaAs QDs by molecular beam epitaxy (MBE) [10–12]. Studies of the physical properties of the grown nanostructures have shown that they are efficient and directional sources of single photons in the wavelength range of 750−800 nm, which indicates the promise of their application for quantum cryptography and the integration of III−V materials with a silicon platform [13–15]. Nevertheless, to increase the number of applications based on NWs with QDs, it is necessary to expand the range of materials composing QDs and NWs. This will lead to the advancement of single-photon sources to the long-wavelength region.

In this work, the results of experimental studies of the synthesis by the MBE method and the physical properties of AlGaAs NWs with InGaAs QDs on the silicon surface are presented. Unlike the most studied nanostructures in the InGaAs/GaAs [16–19] material system, the localization of charge carriers in InGaAs QDs in the AlGaAs NW body has a higher value, since the AlGaAs band gap exceeds the analogous parameter GaAs. This can lead to increase in temperature at which one-photon properties of QDs can be observed.

2. Experimental methods

Experiments on the synthesis of AlGaAs NWs with InGaAs QDs were performed using a Riber Compact 21 MBE setup equipped with indium (In), gallium (Ga), aluminum (Al), arsenic (As) effusion sources and an additional metallization chamber. At the preparatory stage, polished Si(111) wafers were subjected to cleaning in an aqueous solution of HF(1 : 10). Then the substrates were loaded into the metallization chamber, heated up to 950°C and kept at this temperature for 20 min to remove the residual oxide. At the next stage, the substrate temperature was lowered to 550°C, and thin layer of gold (1−2 nm) was

deposited onto the substrate surface, followed by minute exposure at the same temperature to form catalyst droplets for subsequent growth of NWs. After cooling to room temperature, the substrates were transferred to the growth chamber without violating the ultrahigh vacuum conditions. Then the substrate temperature was raised to the growth temperature (510°C). The temperature of the substrates did not change during the entire growth process. After stabilization of the substrate temperature, the shutters of the Al, Ga, and As sources were simultaneously opened for 13 min to form AlGaAs NWs. For the subsequent formation of InGaAs QDs, the Al source shutter was closed and, at the same time, the In source shutter was opened for 5 s. At the final stage of growth, the shutter of the Al source was opened again to form the upper part of the AlGaAs NWs. According to preliminary calibrations, the fluxes from Al and Ga sources corresponded to the growth rate of the AlGaAs layer i.e. 1 monolayer per second (MS/s), the nominal compositions of the AlGaAs and InGaAs solid solutions were 0.3 for Al and 0.5 for In, respectively.

The morphological properties of the synthesized nanostructures were studied by scanning electron microscopy (SEM). The structural properties of the synthesized nanostructures were studied by transmission electron microscopy (TEM) with the possibility of energy dispersive X-ray analysis (EDX). The optical properties of the grown samples were studied using the micro-photoluminescence (micro-PL) method at temperature of 4 K. To compare the emission from nanostructures grown in different directions, part of the NWs standing on the substrate was removed from the surface and placed on the surface of a clean Si/SiO_x wafer.

3. Results and discussion

Fig. 1 shows a typical SEM image of grown AlGaAs NWs with InGaAs QDs on silicon surface. It can be seen from the figure that NWs have a conical shape with average height of 1.4 μm. The NW diameter was 150 nm at the base and 30 nm at the top, with average surface density of NWs $\sim 9 \cdot 10^8$ cm^{-2}. It should be noted that NWs formed predominantly in the $\langle 111 \rangle$ direction, which indicates their epitaxial growth on the Si(111) substrate. This was achieved through a unique procedure for depositing gold in a separate metallization chamber and transferring the substrate to the growth chamber without violating ultrahigh vacuum conditions. Otherwise, due to the rapid formation of a natural oxide layer on the substrate surface, it must be additionally removed in the growth station at a sufficiently high substrate temperature ($\sim$ 950°C), which can lead to uncontrolled etching at the substrate interface and disruption of the epitaxial bond with the substrate.

Typical TEM image of a single AlGaAs NW with InGaAs QDs dispersed onto carbon grid is shown in Fig. 2. It can be seen from the Figure that, as in the case of the InP/InAsP [8] materials system, the formation of mainly

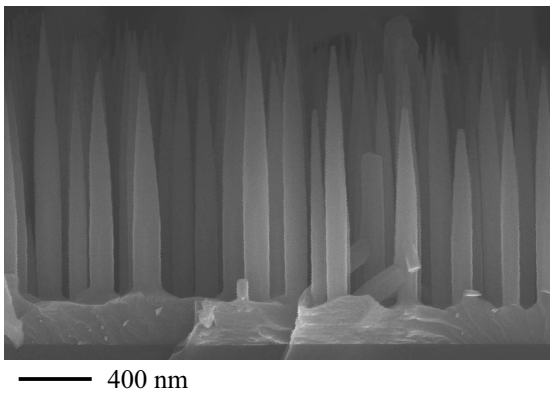

Figure 1. Typical SEM image of grown AlGaAs NWs with InGaAs QDs on a silicon surface.

Figure 2. Typical TEM image of a single AlGaAs NW with InGaAs QD dispersed onto a carbon grid.

two objects is observed in the NW body: InGaAs QDs due to axial growth and InGaAs QWs due to radial growth. With QD formation time equal to 5 s, its dimensions are on average $\sim$ 21 nm in height and $\sim$ 11 nm in diameter. Studies of the compositions of InGaAs nanoobjects by the EDX method showed that the molar fraction of indium in the solid solution is the same for both QDs and QWs and amounts to $\sim$ 20%. It is important to note that the synthesized nanostructures have a predominantly wurtzite crystallographic phase [10]. Nanostructures with a wurtzite crystallographic phase may be promising for a number of applications, for example, piezoelectric generators [20–22]. Nevertheless, the wurtzite structures of both NWs and QDs contain rare inclusions of the cubic phase of the material, which should not significantly affect the optical properties

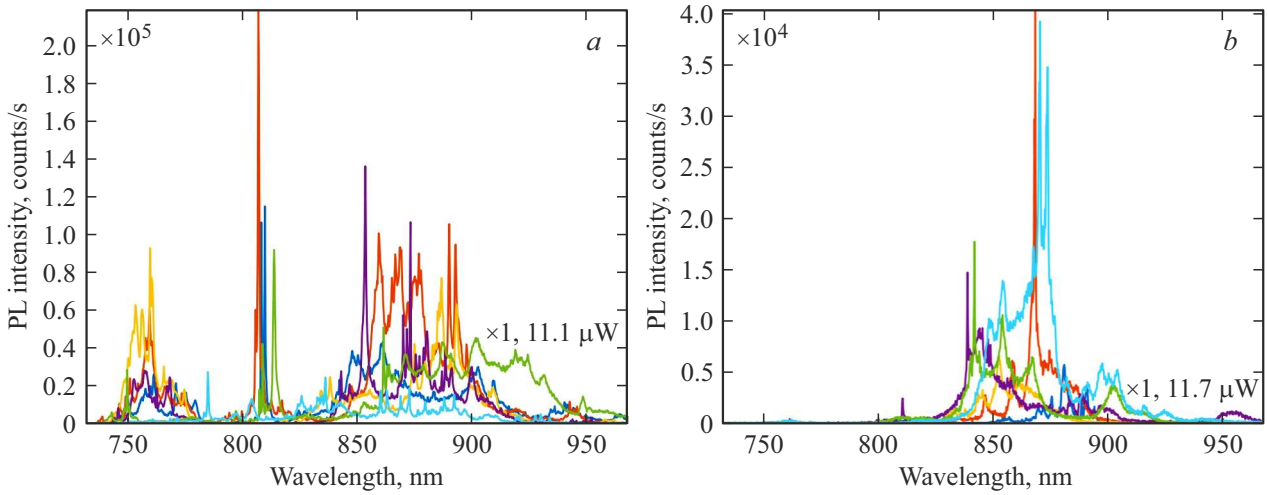

Figure 3. Sets of typical micro-PL spectra at temperature of 4 K from AlGaAs NWs with InGaAs QD: *a* of standing ones on the Si surface; *b* of lying ones on the Si/SiO_x surface. (A color version of the figure is provided in the online version of the paper).

of QDs More detailed theoretical and experimental studies of the formation of crystallographic phase transitions near QDs will be carried out in subsequent works.

Fig. 3, *a* and *b* show sets of typical micro-PL spectra measured at different points of the sample at temperature of 4 K, obtained from standing on a Si substrate (Fig. 3, *a*) and AlGaAs lying on a Si/SiO_x substrate (Fig. 3, *b*) NWs with InGaAs QDs. Should be noted that when the laser spot was focused to the size of $\sim 1\,\mu$m and the surface density of the grown nanostructures was high, about 10–20 NWs with QDs were simultaneously excited. As can be seen from Fig. 3, the micro-PL spectra clearly show three main bands: (*1*) in the 750 nm region, corresponding to the emission from AlGaAs NWs [11,12], (*2*) in the 820 nm region, corresponding to radiation from the InGaAs QW, and (*3*) in the 850 to 900 nm range, corresponding to radiation from InGaAs QDs. Nevertheless, the spectra obtained from standing and lying NWs differ significantly from each other. In the case of NWs lying on the surface, radiation from QDs prevails, but no significant signal from AlGaAs NW or InGaAs QW is observed. This correlates well with the theoretical predictions described in [23,24], according to which, for emitters with a longer wavelength, the anisotropy in the radiation is suppressed;therefore, for radiation from InGaAs QDs emitting in the range 850–900 nm, the anisotropy is less pronounced.

4. Conclusion

In the work, the possibility of growing AlGaAs NWs with InGaAs QDs on a silicon surface by the MBE method was demonstrated. The results of studies of the structural and optical properties of the grown nanostructures showed that, as in the case of the InP/InAsP material system, the formation of mainly two objects is observed in the NW body: InGaAs QDs due to axial growth and InGaAs QWs due to radial growth. It is important to note that the grown nanostructures were formed predominantly in the wurtzite crystallographic phase. The results of studies of the physical properties of the grown nanostructures indicate that they are promising for promoting single-photon sources to the long-wavelength region. Thus, this work opens up new prospects for the integration of direct-gap III–V semiconductors with a silicon platform for various applications in the field of photonics and quantum communication technologies.

Funding

The synthesis of experimental samples was carried out with the financial support of the Ministry of Science and Higher Education in the part of the state assignment. No. 0791-2020-0003. The study of the optical properties of grown nanostructures was carried out with the financial support of the European Research Council (ERC) under the European Union's Horizon 2020 research and innovation program (grant agreement No. 101003378). The study of the structural properties of experimental samples was carried out with the financial support of St.-Petersburg State University within the research grant No. 92591131.

Conflict of interest

The authors declare that they have no conflict of interest.

References

[1] M. Karimi, V. Jain, M. Heurlin, A. Nowzari, L. Hussain, D. Lindgren, J.E. Stehr, I.A. Buyanova, A. Gustafsson, L. Samuelson. Nano Lett., **17** (6), 3356 (2017).
[2] J.K. Hyun, S. Zhang, L.J. Lauhon. Ann. Rev. Mater. Sci., **43**, 451 (2013).

[3] K.W. Ng, W.S. Ko, T.-T.D. Tran, R. Chen, M.V. Nazarenko, F. Lu, V.G. Dubrovskii, M. Kamp, A. Forchel, C.J. Chang-Hasnain. ACS Nano, **7** (1), 100 (2013).
[4] M. Heiss, Y. Fontana, A. Gustafsson, G. Wüst, C. Magen, D.D. O'regan, J.W. Luo, B. Ketterer, S. Conesa-Boj, A.V. Kuhlmann, J. Houel, E. Russo-Averchi, J.R. Morante, M. Cantoni, N. Marzari, J. Arbiol, A. Zunger, R.J. Warburton, A. Fontcuberta I Morral. Nature Materials, **12** (5), 439 (2013).
[5] K.S. Leschkies, R. Divakar, J. Basu, E. Enache-Pommer, J.E. Boercker, C.B. Carter, U.R. Kortshagen, D.J. Norris, E.S. Aydil. Nano Lett., **7** (6), 1793 (2007).
[6] A.V. Akimov, A. Mukherjee, C.L. Yu, D.E. Chang, A.S. Zibrov, P.R. Hemmer, H. Park, M.D. Lukin. Nature, **450** (7168), 402 (2007).
[7] M.T. Borgström, V. Zwiller, E. Müller, A. Imamoglu. Nano Lett., **5** (7), 1439 (2005).
[8] R.R. Reznik, G.E. Cirlin, I.V. Shtrom, A.I. Khrebtov, I.P. Soshnikov, N.V. Kryzhanovskaya, E.I. Moiseev, A.E. Zhukov. Techn. Phys. Lett., **44** (2), 112 (2018).
[9] V.G. Dubrovskii, G.E. Cirlin, V.M. Ustinov. Phys. Rev. B, **68** (7), 075409 (2003).
[10] L. Leandro, R. Reznik, J.D. Clement, J. Repän, M. Reynolds, E.V. Ubyivovk, I.V. Shtrom, G. Cirlin, N. Akopian. Sci. Rep., **10** (1), 1 (2020).
[11] G.E. Cirlin, I.V. Shtrom, R.R. Reznik, Y.B. Samsonenko, A.I. Khrebtov, A.D. Bouravleuv, I.P. Soshnikov. Semiconductors, **50** (11), 1421 (2016).
[12] G.E. Cirlin, R.R. Reznik, I.V. Shtrom, A.I. Khrebtov, I.P. Soshnikov, S.A. Kukushkin, L. Leandro, T. Kasama, N. Akopian. J. Phys. D, **50** (48), 484003 (2017).
[13] L. Leandro, C.P. Gunnarsson, R. Reznik, K.D. Jöns, I. Shtrom, A. Khrebtov, T. Kasama, V. Zwiller, G. Cirlin, N. Akopian. Nano Lett., **18** (11), 7217 (2018).
[14] L. Leandro, J. Hastrup, R. Reznik, G. Cirlin, N. Akopian. NPJ Quant. Inf., **6** (1), 1 (2020).
[15] R.R. Reznik, K.M. Morozov, I.L. Krestnikov, K.P. Kotlyar, I.P. Soshnikov, L. Leandro, N. Akopian, G.E. Cirlin. Techn. Phys. Lett., 1 (2021).
[16] M. Heiss, B. Ketterer, E. Uccelli, J.R. Morante, J. Arbiol, A.F. i Morral. Nanotechnology, **22** (19), 195601 (2011).
[17] J. Tatebayashi, S. Kako, J. Ho, Y. Ota, S. Iwamoto, Y. Arakawa. J. Cryst. Growth, **468**, 144 (2017).
[18] J. Tatebayashi, Y. Ota, S. Ishida, M. Nishioka, S. Iwamoto, Y. Arakawa. Appl. Phys. Lett., **105** (10), 103104 (2014).
[19] M.N. Makhonin, A.P. Foster, A.B. Krysa, P.W. Fry, D.G. Davies, T. Grange, T. Walther, M.S. Skolnick, L.R. Wilson. Nano Lett., **13** (3), 861 (2013).
[20] C.T. Huang, J.H. Song, C.M. Tsai, W.F. Lee, D.H. Lien, Z.Y. Gao, Y. Hao, L.J. Chen, Z.L. Wang. Adv. Mater., **36**, 4008 (2010).
[21] N. Gogneau, N. Jamond, P. Chretien, F. Houze, E. Lefeuvre, M. Tchernycheva. Semicond. Sci. Technol., **31** (10), 103002 (2016).
[22] P.A. Alekseev, V.A. Sharov, P. Geydt, M.S. Dunaevskiy, V.V. Lysak, G.E. Cirlin, R.R. Reznik, A.I. Khrebtov, I.P. Soshnikov, E. Lähderanta. Phys. Status Solidi: Rapid Res Lett., **12** (1), 1700358 (2018).
[23] A. Kuznetsov, P. Roy, V.M. Kondratev, V.V. Fedorov, K.P. Kotlyar, R.R. Reznik, A.V. Vorobyev, I.S. Mukhin, G.E. Cirlin, A.D. Bolshakov. Nanomaterials, **12** (2), 241 (2022).
[24] R.R. Reznik, G.E. Cirlin, K.P. Kotlyar, I.V. Ilkiv, N. Akopian, L. Leandro, V.V. Nikolaev, A.V. Belonovski, M.A. Kaliteevski. Nanomaterials, **11** (11), 2894 (2021).